

PAPER IV

TEIR, S., REVITZER, H., ELONEVA, S., FOGELHOLM, C-J., ZEVENHOVEN, R., 2007.

Dissolution of natural serpentinite in mineral and organic acids.

International Journal of Mineral Processing, 83(1-2), 36-46.

© 2007 Elsevier B.V.

Reprinted with permission.

Dissolution of natural serpentinite in mineral and organic acids

Sebastian Teir^{a,*}, Hannu Revitzer^b, Sanni Eloneva^a,
Carl-Johan Fogelholm^a, Ron Zevenhoven^c

^a *Laboratory of Energy Engineering and Environmental Protection, Helsinki University of Technology, PO. Box 4400, FIN-02015 TKK, Finland*

^b *Laboratory of Physical Chemistry and Electrochemistry, Helsinki University of Technology, PO. Box 6100, FIN-02015 TKK, Finland*

^c *Heat Engineering Laboratory, Åbo Akademi University, Piispankatu 8, FIN-20500 Turku, Finland*

Received 9 November 2006; received in revised form 18 December 2006; accepted 5 April 2007

Available online 19 April 2007

Abstract

Abundant resources of magnesium silicates make an interesting prospect for long-term storage of CO₂ by mineral carbonation. Several carbonation processes proposed in literature for CO₂ storage employ extraction of silicate minerals using a liquid solvent. In this study, the dissolution of natural serpentinite in respective solutions of acids, bases and ammonium salts has been investigated. Experiments performed at room temperature showed that H₂SO₄ was most efficient at extracting magnesium from serpentinite, followed by HCl, HNO₃, HCOOH and CH₃COOH. Experiments for determining the dissolution kinetics was performed at temperatures of 30, 50 and 70 °C in 2 M solutions of H₂SO₄, HCl, and HNO₃. At 70 °C temperatures all magnesium was extracted from serpentinite in each of the three acid solutions tested during 1–2 h. Also a large part of iron in serpentinite was extracted, while very little silicon dissolved (<4%). The dissolution rate seemed to be limited by product layer diffusion for serpentinite particles with a size distribution of 74–125 μm. The apparent activation energies were 68 kJ mol⁻¹ for dissolution in H₂SO₄, 70 kJ mol⁻¹ for dissolution in HCl, and 74 kJ mol⁻¹ for dissolution in HNO₃.

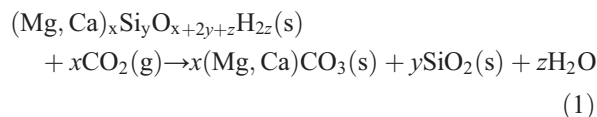
© 2007 Elsevier B.V. All rights reserved.

Keywords: Serpentinite; Serpentine; Mineral carbonation; Extraction; Kinetics; Leaching

1. Introduction

Carbon dioxide capture and storage (CCS) is considered as one of the main options for reducing atmospheric emissions of CO₂ from human activities. This concept includes capture (separation and compression) of CO₂ from large, centralized CO₂ emitters (such as power plants, metal industry, and cement producers), and transportation to a suitable storage site (such as depleted oil and gas fields or saline aquifers). Carbonation of natural silicate minerals is an interesting alternative to geological reservoirs for storage of CO₂.

Alkaline-earth oxides, such as magnesium oxide (MgO) and calcium oxide (CaO), are present in large amounts and high concentrations in naturally occurring silicate minerals such as serpentine and olivine (Goff and Lackner, 1998). Carbonation of these minerals traps CO₂ as environmentally stable carbonates (Goldberg et al., 2001):



Since carbonation securely traps CO₂ there would be little need to monitor the disposal sites and the environmental risks would be very low (IPCC, 2005). Silicate

* Corresponding author. Tel.: +358 9 4513631; fax: +358 9 4513418.
E-mail address: sebastian.teir@tkk.fi (S. Teir).

mineral resources have also the highest capacity and longest storage time of CO₂ of the storage options currently known (Lackner, 2003). The natural carbonation of silicate minerals is very slow, which means that the carbonation reaction must be accelerated considerably to be a viable large-scale storage method for captured CO₂.

In Finland, the most common rocks rich in magnesium are ultramafic rocks, of which serpentinites are the most interesting for CCS purposes, consisting mainly of serpentine. The known and accessible resources of serpentinite in Eastern Finland alone could theoretically be sufficient for 200–300 years of CCS processing, if 10 Mt CO₂ per year is stored (Teir et al., 2006). Serpentinites are already being mined simultaneously with industrial minerals and metals (such as talc, soap stone, chromium and nickel), after which they are piled as barren rock or dammed as tailings.

The most efficient processes suggested for carbonation involve leaching or dissolution of silicates in liquid media and precipitation of magnesium or calcium as carbonates or hydroxides for subsequent carbonation (Huijgen and Comans, 2003, 2005). Mineral acids (Lackner et al., 1995; Park et al., 2003; Maroto-Valer et al., 2005), organic acids and ligands (Park et al., 2003), as well as caustic soda (Blencoe et al., 2004) have been suggested for dissolving serpentine for subsequent carbonation. Most of these processes have been considered too expensive for CO₂ storage, since they require energy (for crushing, grinding or preheating) and possibly chemical additives that cannot be recovered. However, the available experimental data on these processes is scarce and occasionally contradicting.

The present study was aimed at finding a suitable solvent for extracting magnesium from Finnish serpentinite tailings for subsequent fixation of CO₂ by precipitation of magnesium carbonates. After comparing the magnesium extraction potential by dissolving serpentinite in various acid, base, and salt solutions, the dissolution kinetics was studied in more detail in hydrochloric acid, sulfuric acid, and nitric acid. Although comprehensive kinetic studies are available, most of these have involved energy intensive pretreatments of the ore by high-temperature roasting (Fouda et al., 1996a,b; Apostolidis and Distin, 1978). Since pretreatment of magnesium silicate would make a subsequent carbonation process more expensive, this study focus on dissolution of untreated, ground, serpentinite at relatively low temperatures (20–70 °C). A future paper will address the carbonation of the extracted magnesium.

2. Materials and methods

2.1. Characterization of serpentinite sample

Serpentinite from the stockpile of the Hitura nickel mine of Outokumpu Mining Oy, central Finland, was selected for experimental study. A batch of 7 kg serpentinite rocks was ground and sieved, from which a particle size fraction of 74–125 µm was selected for the experiments. Samples of the both the sieved 74–125 µm fraction and the unsieved fraction were analyzed using X-Ray Diffraction (XRD) and X-Ray Fluorescence Spectroscopy (XRF). For a more accurate measurement of the contents of elements in the serpentinite, five samples of the sieved fraction were completely dissolved using a solution of HCl, H₃PO₄, and HF, from which surplus HF was eliminated using saturated boric acid (H₃BO₃). The solutions were analyzed with Inductively Coupled Plasma-Atomic Emission Spectrometry (ICP-AES) using two different wave lengths to give a more exact reference number for the concentrations of Mg, Si, Fe, Ca, Al, Ni, Mn, Cr, Cu, Co, and Ba in serpentinite. The carbonate (CO₃) content of serpentinite was determined using a Shimadzu 5000A Total Organic Carbon (TOC) analyzer, while the loss on ignition was determined by drying the sample at 970 °C for 1 h.

2.2. Selection of solvents

In order to find a suitable solvent for leaching magnesium from serpentine, common acids used in mineral processing (HCl, H₂SO₄, HNO₃) were tested alongside two common weak acids (HCOOH and CH₃COOH). Although acids are known to extract magnesium from magnesium silicates, bases can dissolve silicates too and favor the formation of carbonates. Promising results have also recently been reported with dissolution of steelmaking slags in ammonium salts (Yogo et al., 2004). Therefore, dissolution of serpentinite was also tested in solutions of NaOH, KOH, NH₃, NH₄Cl, (NH₄)₂SO₄, and NH₄NO₃. A batch of 1 g of serpentinite (74–125 µm) was dissolved in separate 50 ml aqueous solutions of 1 M, 2 M and 4 M concentrations of respective solvent in a sealed Erlenmeyer flask. The solutions were stirred at 1000 rpm at a room temperature of 20 °C. The solutions were immediately filtered with 0.45 µm Pall GxP syringe filters 1 h after the addition of serpentinite. The concentrations of Mg, Fe, and Si in the filtered solutions were measured with ICP-AES using two different wave lengths to give more exact results.

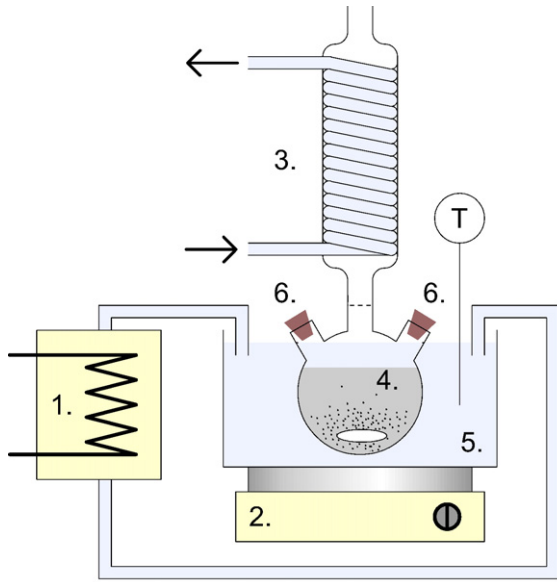


Fig. 1. Dissolution experiment setup: 1 — temperature-controlled bath with external flow; 2 — magnetic stirrer; 3 — tap water-cooled condenser; 4 — glass reactor; 5 — water bath; 6 — outlets for batch addition and solution sampling.

2.3. Dissolution rate of serpentinite in selected solvents

Experiments for determining the dissolution rate of serpentinite in selected solvents were carried out in an open spherical glass batch reactor (500 ml) heated by a temperature-controlled water bath (Fig. 1) and equipped with a water-cooled condenser to minimize solution losses due to evaporation. The solutions were well mixed using a magnetic stirrer set to 600–700 rpm. 500 ml of the desired solution (2 M) was added to the reaction

vessel. With the temperature set to 30 °C, 50 °C, or 70 °C a charge of 10 g of serpentinite was added to the reactor. The solution temperature was verified prior to the batch addition using a mercury thermometer (± 0.2 °C) and the temperature of the bath was constantly monitored. Samples (5 ml per sample) of the solution were extracted with a syringe 5 min prior to charging the reactor, as well as 5 min, 15 min, 30 min, 1 h, 1.5 h, and 2 h after adding the batch to the reactor. The samples were immediately after extraction filtered with 0.45 μm Pall GxF syringe filters. The Mg, Fe and Si concentrations of the samples were measured using ICP-AES. The reactor was weighed before and after the experiments. Each sample extracted, as well as the serpentinite batch added to the solution, was also weighed. Mass balance calculations showed that the loss of mass during the experiments was 0.2–0.7 wt.%. The highest losses were accounted for the experiments performed at 70 °C, which indicates that the losses were mostly due to evaporation.

The results from the ICP-AES analyses showed the concentrations ($c_{i,j}$) of dissolved magnesium, iron, and silicon in the samples extracted during the course of the experiments. In order to compensate for the loss of solution volume ($V_{\text{initial}}=0.5$ l) due to sampling ($V_{\text{sample}}=0.005$ l), the dissolved fraction of a specific element i (magnesium, iron, or silicon) in sample j was calculated as follows:

$$X_{i,j} = \frac{c_{i,j} V_j'}{m'_{i,j}} = \frac{c_{i,j} [V_{\text{initial}} - V_{\text{sample}}(j-1)]}{m_{\text{batch}} \frac{m_i}{m} - V_{\text{sample}} \sum_2^{j-1} c_{i,j}} \quad (2)$$

V_j' is the volume of the solution and $m'_{i,j}$ is the total mass of element i in the reactor prior to the j th sample. The first

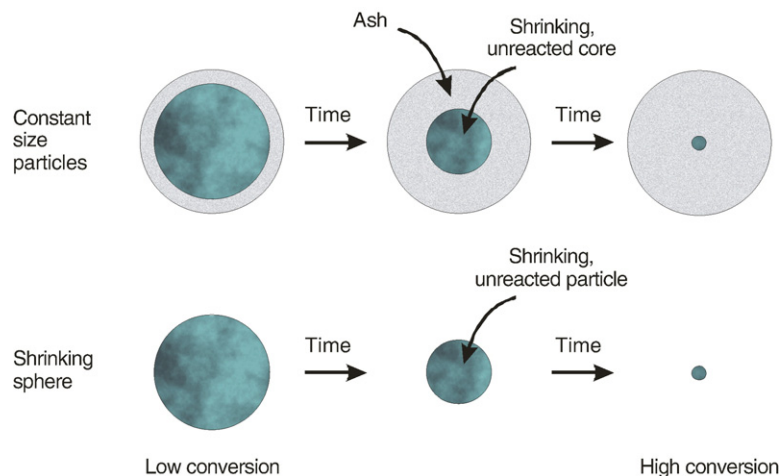


Fig. 2. According to the unreacted-core models the reaction proceeds at a narrow front, which moves into the solid particle. The reactant is completely converted as the front passes by (Levenspiel, 1972).

Table 1

Elemental analysis of serpentinite, 74–125 μm (only concentrations $>0.1 \text{ mg g}^{-1}$ included from XRF-analysis)

Element	m_i/m [mg g^{-1}]	Method
Mg	218	ICP-AES
Si	116 ^a	ICP-AES
Fe	101	ICP-AES
S	4.8	XRF
Ca	3.4	ICP-AES
Cl	2.1	XRF
Al	0.208	ICP-AES
Ni	0.205	ICP-AES
Ti	0.18	XRF
Mn	0.084	ICP-AES
Cr	0.074	ICP-AES
Cu	0.069	ICP-AES
Co	<0.015	ICP-AES
Ba	<0.005	ICP-AES

^a The Si content was 188 mg g^{-1} according to XRF analyses. Although the ICP-AES value was used for calculating Si extraction efficiencies, the actual content of Si is probably somewhere between the two values.

sample was performed 5 min prior to addition of the serpentinite batch ($m_{\text{batch}}=10.0 \text{ g}$) and does not affect the total mass of iron or magnesium in the reactor.

2.4. Kinetic analysis

In order to design a carbonation process, which recovers magnesium ions needed for fixation of CO_2 through dissolution of serpentinite, kinetic data is needed. Heterogeneous fluid–solid reactions may be represented by:



In these reactions, the reaction rate is generally controlled by one of the following steps: diffusion through

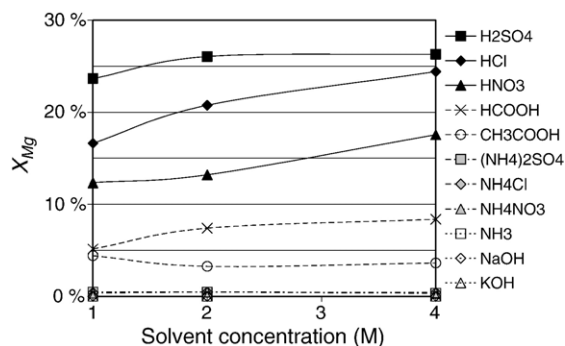


Fig. 4. Fraction of Mg extracted from serpentinite (74–125 μm) in 1 M, 2 M and 4 M concentrations of solvent (1 h, 20 °C).

the fluid film, diffusion through the ash (or solid product) layer on the particle surface, or the chemical reaction at the reaction surface (Levenspiel, 1972). The rate of the process is controlled by the slowest of these sequential steps.

In order to determine the kinetic parameters and rate-controlling step in dissolution of serpentinite in selected mineral acids, the experimental data was analyzed according to the integral analysis method (Levenspiel, 1972). Experimental data were fitted into integral rate equations for unreacted-core models of unchanging size and shrinking size (i.e. product layer stays on particle or is removed, see Fig. 2). Rate equations tested were film diffusion control, product layer diffusion control, and reaction control for constant size particles (flat plate, cylinder, sphere) and shrinking particles (small and large spheres). The multiple regression correlation coefficients (R^2) were calculated for each equation and checked graphically. Experimental data corresponding to $X > 95\%$ were not included in the kinetic analysis, since several

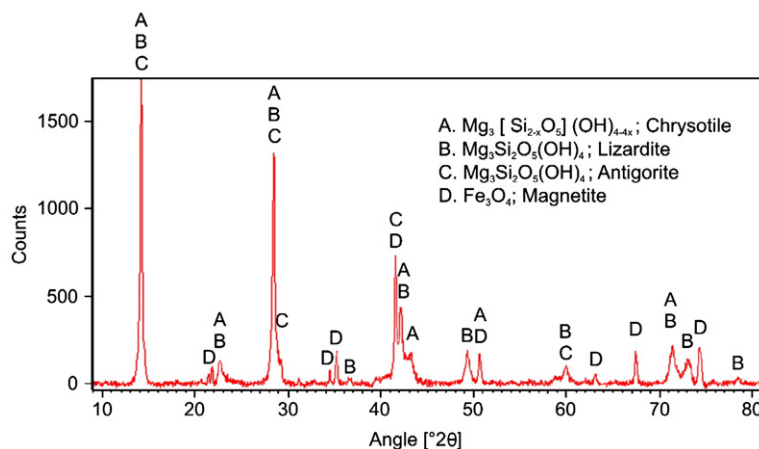


Fig. 3. X-Ray diffractogram of the sieved (74–125 μm) serpentinite.

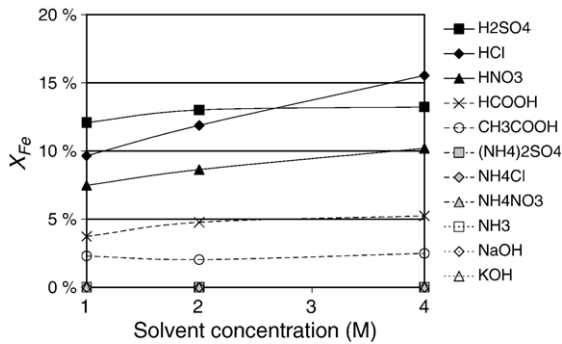


Fig. 5. Fraction of Fe extracted from serpentinite (74–125 μm) in 1 M, 2 M and 4 M concentrations of solvent (1 h, 20 °C).

integral rate equations are not defined at $X=100\%$ and very sensitive to data inaccuracies for conversion values close to $X=100\%$.

3. Results and discussion

3.1. Characterization of serpentinite sample

A summary of the results from the serpentinite dissolution analyses (ICP-AES) and XRF-analysis of the sieved sample is shown in Table 1. The sieved fraction was very similar to the unsieved sample in respect to composition and crystal structure. The XRD pattern (see Fig. 3) of the serpentinite reveals that the rock contained serpentine, ($Mg_3Si_2O_5(OH)_4$; chrysotile, lizardite and antigorite) and magnetite (Fe_3O_4). According to the TOC analysis the serpentinite contained no carbonate (<0.1 wt.%). The loss on ignition at 970 °C was 12 wt.%. Major impurities were S, Ca, and Cl (concentrations of 0.2–0.4 wt.%). Assuming that all magnesium exists as serpentine and all iron as magnetite, the serpentinite would (based on the magnesium and iron fractions of the sample, listed in Table 1) consist of 83 wt.% serpentine and 14 wt.% magnetite.

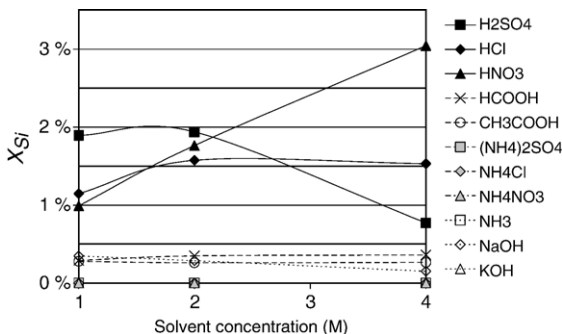


Fig. 6. Fraction of Si extracted from serpentinite (74–125 μm) in 1 M, 2 M and 4 M concentrations of solvent (1 h, 20 °C).

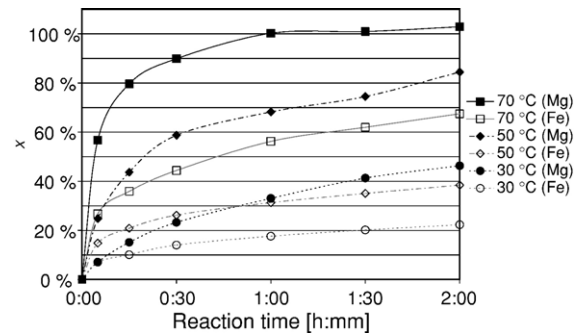


Fig. 7. Effect of temperature on extraction of Mg and Fe from serpentinite (74–125 μm) in 2 M HCl.

3.2. Selection of solvents

The effect of solvent concentration on dissolution of serpentinite in respective solvents is shown in Figs. 4–6. Since the serpentinite contained very low concentrations of other metals, only the concentrations of magnesium, iron and silicon extracted were measured with ICP-AES. The results are shown as mass of element dissolved in solution per mass of element in serpentinite (according to Table 1). All acids tested (CH_3COOH , H_2SO_4 , HCl, HNO_3 and $HCOOH$) were able to extract a significant amount (3–26%) of magnesium from serpentinite in 1 h. None of the acids tested extracts Mg selectively from serpentinite: also Fe (2–16%) and some Si (0–3%) was extracted. However, the silicon concentration in the filtrate may not be an accurate measurement for how much silicon has dissolved, because part of the silica can precipitate as gel on the filter and, thus, reduce the silicon concentration in the filtrate (Teir et al., 2007). According to the results presented in Fig. 4 the solutions of H_2SO_4 were most efficient at extracting magnesium from serpentinite, followed by HCl, HNO_3 , $HCOOH$ and CH_3COOH (listed in order of descending magnesium extraction efficiency). Higher acid concentrations resulted in slightly

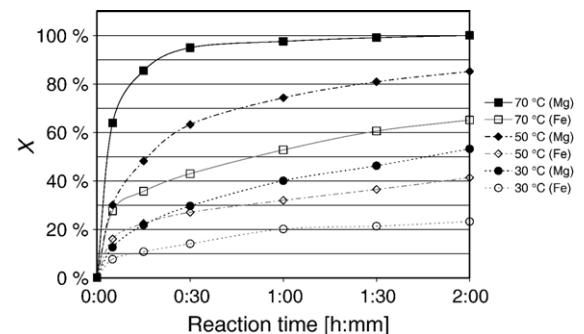


Fig. 8. Effect of temperature on extraction of Mg and Fe from serpentinite (74–125 μm) in 2 M H_2SO_4 .

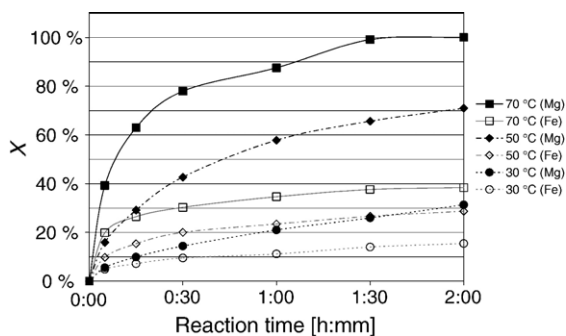


Fig. 9. Effect of temperature on extraction of Mg and Fe from serpentine (74–125 μm) in 2 M HNO₃.

more magnesium and iron ions dissolved, except for the solutions of CH₃COOH, which behaved more irregularly.

The ammonium salt solutions tested (NH₄Cl, (NH₄)₂SO₄, and NH₄NO₃) extracted only 0.3–0.5% of magnesium in serpentine during 1 h. However, the ammonium salt solutions were the only solvents tested that seemed to extract magnesium selectively: no measurable iron or silicon concentration was found in the salt solutions after filtration.

Another interesting result is that no measurable amount of magnesium or iron (<0.05% extracted) had dissolved after 1 h in any of the alkaline solutions tested (NaOH, KOH, and NH₃). No more than 0.3% of the silicon in serpentine was extracted using 4 M solutions of bases. It is likely that a much longer residence time is required for any significant extraction of magnesium in alkaline solutions. The slow dissolution of serpentine in alkaline solutions may be one reason why the carbonation process presented by Blencoe et al. (2004) requires a reaction time of 72 h.

3.3. Dissolution rate of serpentine in selected solvents

Based on the results from the experiments described above, HNO₃, HCl, and H₂SO₄ were selected for further

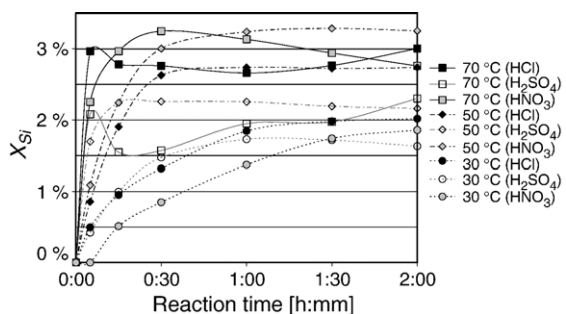


Fig. 10. Effect of temperature on extraction of Si from serpentine (74–125 μm) in 2 M HCl, 2 M H₂SO₄, and 2 M HNO₃.

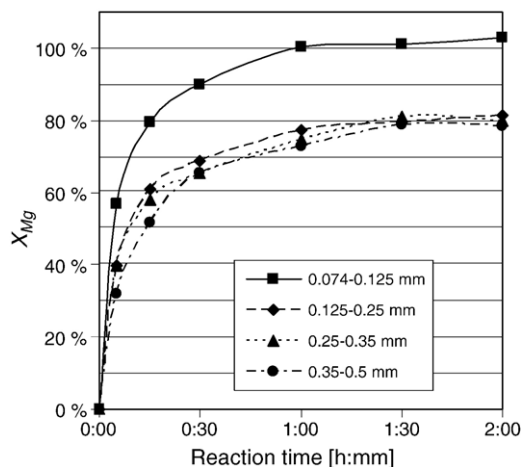


Fig. 11. Effect of particle size on extraction of Mg from serpentine in 2 M HCl at 70 °C.

studies. The dissolution rate of serpentine with a particle size fraction of 74–125 μm was tested in 2 M concentrations of HNO₃, HCl, and H₂SO₄, respectively, using solution temperatures of 30 °C, 50 °C, and 70 °C. The effect of temperature upon the dissolution of serpentine is shown in Figs. 7–10. As can be seen from the figures, higher temperatures yield higher reaction rates for each acid tested. At 70 °C all acids were able to leach 100% of magnesium in serpentine in 2 h, while simultaneously 38–67% of iron in serpentine was extracted (Figs. 7–9). However, only 3% of silicon in serpentine was dissolved (Fig. 10). Apparently, magnesium and iron are extracted leaving behind mostly silica and small quantities of magnetite. While nitric acid was slower at dissolving serpentine than the other acids, it was more selective on extracting magnesium at 70 °C.

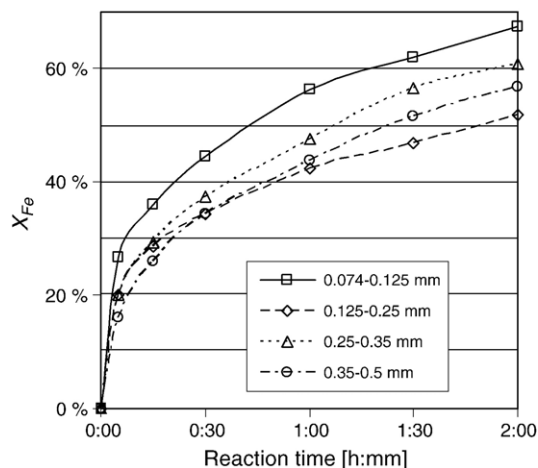


Fig. 12. Effect of particle size on extraction of Fe from serpentine in 2 M HCl at 70 °C.

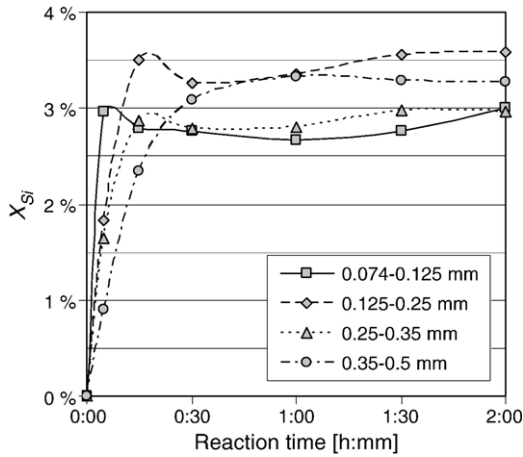


Fig. 13. Effect of particle size on extraction of Si from serpentine in 2 M HCl at 70 °C.

The effect of the particle size was tested in 2 M HCl at 70 °C solution temperature, using sieved serpentine fractions of 74–125 μm , 125–250 μm , 250–350 μm , and 350–500 μm (Figs. 11–13). Five minutes after the addition of serpentine, smaller particle sizes yielded a higher extraction of all the elements analyzed for (Mg, Fe, Si). This trend continued for the extraction of iron throughout the experiment, except for the experiment with particle size fraction 125–250 μm , which gave the lowest extraction rate of iron of the particle size fractions tested. Extraction of magnesium and iron (Figs. 11–12) was most effective using the fraction of serpentine with the smallest particle sizes (74–125 μm). However, particle size did not seem to have a significant effect on magnesium extraction from the other fractions tested: fractions of 125–250 μm , 250–350 μm , and 350–500 μm gave almost equal magnesium extraction rates, settling at 78–81% extraction after 1–2 h. The maximum amount of Si extracted in solution appeared to be independent of tested particle size (see Fig. 13).

3.4. Kinetic analysis

Kinetic analysis was performed based on experimental data for dissolution of magnesium from serpentine

Table 2
Multiple regression coefficients for experimental kinetic data fitted to unreacted-core models of constant size spherical particles

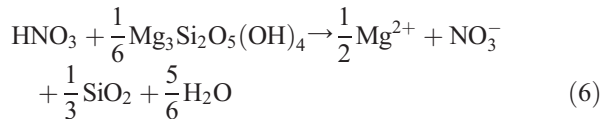
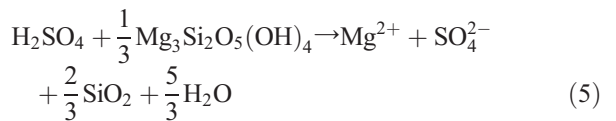
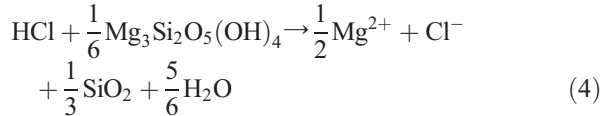
Model	Equation	$R^2_{\min}-R^2_{\max}$
Product layer diffusion	$kt=1-3(1-X_B)^{2/3}+2(1-X_B)$	0.936–0.998
Chemical reaction controls	$kt=1-(1-X_B)^{1/3}$	0.661–0.901
Film diffusion	$kt=X_B$	–0.760–0.863

Table 3

Multiple regression coefficients for experimental kinetic data fitted to unreacted-core models of small shrinking spherical particles

Model	Equation	$R^2_{\min}-R^2_{\max}$
Chemical reaction controls	$kt=1-(1-X_B)^{1/3}$	0.661–0.901
Film diffusion	$kt=1-(1-X_B)^{2/3}$	0.483–0.882

(Figs. 7–9). Since magnesium exists as serpentine ($\text{Mg}_3\text{Si}_2\text{O}_5(\text{OH})_4$) in serpentine, extraction of magnesium in the acids tested can be described in the form of Eq. (3):



According to the regression correlation coefficients calculated (Tables 2 and 3), the experimental data was best fitted towards the integral rate equation for product layer diffusion (Figs. 14–16):

$$t = \frac{\rho_B r^2}{6bD_e C_A} \left[1 - 3(1 - X_B)^{2/3} + 2(1 - X_B) \right] = \frac{1}{k} \left[1 - 3(1 - X_B)^{2/3} + 2(1 - X_B) \right] \quad (7)$$

However, the equation does not perfectly match the points derived from the experimental data. The positive deviation,

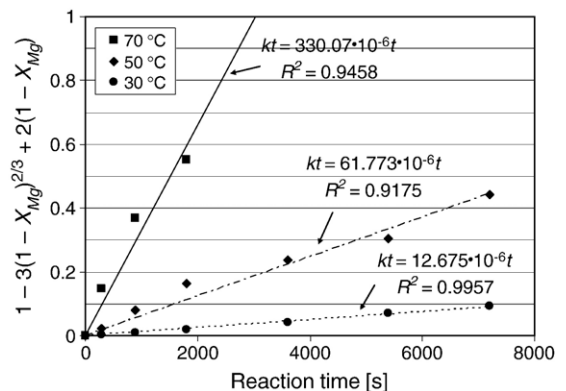


Fig. 14. $1-3(1-X_{\text{Mg}})^{2/3}+2(1-X_{\text{Mg}})$ vs. reaction temperature for extraction of Mg from serpentine in 2 M HCl.

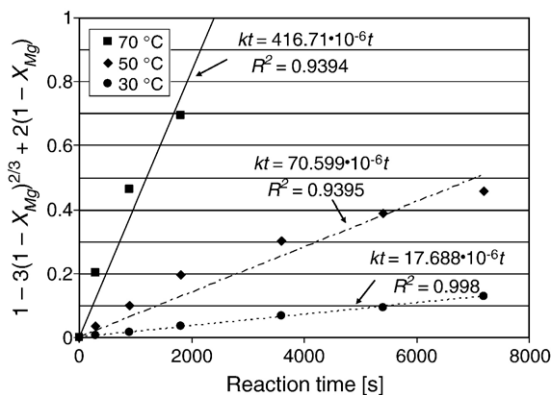


Fig. 15. $1 - 3(1 - X_{Mg})^{2/3} + 2(1 - X_{Mg})$ vs. reaction temperature for extraction of Mg from serpentine in 2 M H_2SO_4 .

observed for the first data points in comparison to the kinetic model (Figs. 14–16), may be explained by the initial build-up of a product layer: at the beginning of the reaction no product is present, but as the reaction proceeds, the product layer builds up (Fig. 2). It may also be partly due to an initial rise in solution temperature of a few degrees, caused by the heat released when serpentine rapidly dissolved. The negative deviation of experimental data fitted to the kinetic model may be due to a decreasing acid concentration at high conversion levels. Assuming serpentine dissolves mainly according to Eqs. (4–6), roughly 80% of HNO_3 , 80% of HCl , or 90% of H_2SO_4 is left after a 100% conversion of 10 g serpentine in 500 ml of 2 M acid. A smaller serpentine batch could have reduced the deviations observed, but then errors due to variation in serpentine composition might have been pronounced instead.

The apparent rate constants were determined from the slope of the lines in Figs. 14–16. The apparent rate

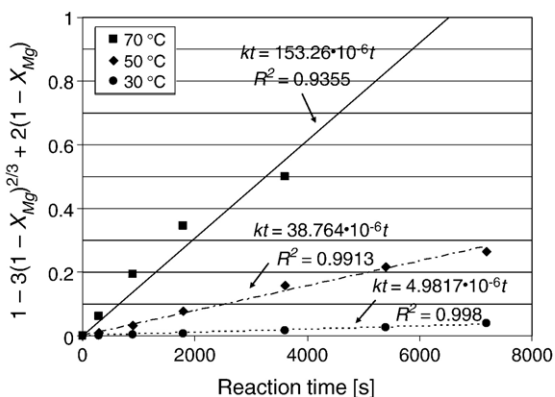


Fig. 16. $1 - 3(1 - X_{Mg})^{2/3} + 2(1 - X_{Mg})$ vs. reaction temperature for extraction of Mg from serpentine in 2 M HNO_3 .

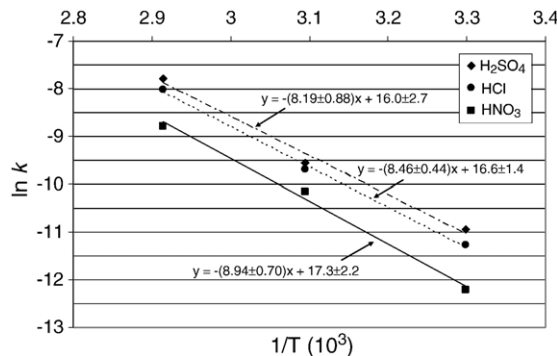


Fig. 17. Arrhenius plot for extraction of Mg from serpentine in 2 M H_2SO_4 , 2 M HCl , or 2 M HNO_3 including standard errors for the coefficients of the trend lines.

constant can be used for determining the temperature dependency by Arrhenius' law:

$$k = k_0 e^{-E/RT} \tag{8}$$

By plotting the apparent rate constants for each experiment in an Arrhenius plot (Fig. 17) the activation energies (E) and the frequency factors (k_0) were determined and the results are shown in Table 4. The activation energy found in the present study for dissolution of serpentine in HNO_3 is similar to that calculated by Fouda et al. (1996b) for dissolution of roasted serpentine ore in HNO_3 (Table 5). The activation energy for dissolution of serpentine in H_2SO_4 is much higher than those reported for dissolution of roasted serpentine ore, but similar to the dissolution of ground, natural olivine (Table 5).

The results (Figs. 14–16) indicate that the rate limiting step for dissolution of serpentine in HCl , H_2SO_4 , and HNO_3 is product layer diffusion. This result is in agreement with Luce et al. (1972), who found that either diffusion of ions in the mineral lattice itself or through a product layer is the rate-controlling mechanism for dissolution of magnesium silicates (serpentine, forsterite and enstatite). Apostolidis and Distin (1978) found that at magnesium extractions above 25% the rate was limited by diffusion through a silica coating attached to

Table 4
Apparent activation energy and frequency factor calculated using the coefficients of the trend lines of the Arrhenius plots in Fig. 17

Solvent	Activation energy E [kJ mol ⁻¹]	Frequency factor k_0 [s ⁻¹]
H_2SO_4	68.1 ± 7.3	8.6 · 10 ⁶
HCl	70.4 ± 3.7	1.6 · 10 ⁷
HNO_3	74.3 ± 5.8	3.4 · 10 ⁷

Table 5
Data on dissolution rates of serpentine from literature

Author	Magnesium silicate properties	Solution properties	Rate limiting step	Activation energy E [kJ mol ⁻¹]
Fouda et al. (1996a)	Serpentine ore (serpentine, iron oxide, aluminum oxide) roasted at 800 °C for 2–3 h	3 M H ₂ SO ₄ , $T=30-75$ °C	Chemical reaction ^a	35.6
Fouda et al. (1996b)	Serpentine ore roasted at 700 °C for 6 h and 825 °C for 2 h	3 M HNO ₃ , $T=30-75$ °C	Chemical reaction ^a	72.8
Apostolidis and Distin (1978)	Ground olivine	0.15–0.6 M H ₂ SO ₄ , $T=30-70$ °C	Chemical reaction ^b ($X_{Mg} < 25\%$)	50.2
Jonckbloedt (1998)	Ground olivine	3 M H ₂ SO ₄ , $T=60-90$ °C	Chemical reaction	66.5±2
Chen and Brantley (2000)	Ground olivine	2 ≤ pH ≤ 5 (HCl) $T=65$ °C	Chemical reaction ^a	126±17 (calculated for pH 0)
Hänchen et al. (2006)	Ground olivine	2 ≤ pH ≤ 8.5 (Cl and LiOH), $T=90-150$ °C	Chemical reaction ^c	52.9±6.9

^a Assumption by respective author(s) based on a relatively high activation energy.

^b For $X_{Mg} > 25\%$ the magnesium extraction rate was found to be limited by a silica coating attached to the silicate particle surface, i.e. product layer diffusion (Apostolidis and Distin, 1978).

^c Surface controlled dissolution was assumed (Hänchen et al., 2006).

the particle surface. The low concentration of dissolved silicon in our experiments supports the theory of a build-up of a product layer of silica on the particles.

For a pure diffusion controlled process, the activation energy should be rather low. However, the results show that the process is very temperature sensitive and the activation energy is of the order of 70 kJ mol⁻¹, which is high for a diffusion controlled process. It is possible that chemical reaction is rate limiting in the beginning of the reaction, with product layer diffusion gradually becoming rate limiting as the product layer of silica builds up and the unreacted surface area decreases. For a chemical reaction with diffusion control, the observed activation energy is roughly one half of that for a pure chemical reaction (Levenspiel, 1972). This suggests that the true activation energy for serpentine dissolution would be of the order of 140–150 kJ mol⁻¹. This is similar to the activation energy for dissolution of olivine as reported by Chen and Brantley (2000) (Table 5), and also consistent with activation energies calculated for dissolution of tetrahedral silicate bridges (Pelmenchikov et al., 2000).

According to Eq. (7), when product layer diffusion controls the reaction rate, the reaction time should be in proportion to the square of the particle radius. This is supported by the experimental observations when comparing the dissolution of serpentinite with a particle size fraction of 74–125 μm to that of 125–250 μm (Fig. 11). However, the reaction conversion curves for the particle size fractions of 125–250 μm is similar to those for particle size fractions 250–350 μm and 350–500 μm. The reason for the independence of conversion with particle size is not clear at the present time, but would suggest that another mechanism may be in play at larger particle sizes.

To further enhance the dissolution rate a grinding media (e.g. fluidization using glass beads) could be used simultaneously to remove the silica layer from the particles (Park and Fan, 2004). Studies have also shown that after roasting serpentine ore at 700–800 °C serpentine decomposes to olivine, which has a higher reactivity than serpentine. For roasted serpentinite and olivine, the dissolution kinetics have been found to follow a shrinking core model, while surface chemical reaction is the rate limiting step (Fouda et al., 1996a,b; Apostolidis and Distin, 1978; Jonckbloedt, 1998; Hänchen et al., 2006). However, heat activation of the mineral increases considerably the energy demand of the process.

4. Conclusions

All acids tested were able to extract a significant amount (3–26%) of magnesium and (2–16% of) iron from serpentinite in 1 h using acid concentrations of 1 M–4 M at room temperature. Sulfuric acid yielded the highest magnesium and iron concentrations, followed by hydrochloric acid, nitric acid, formic acid and acetic acid. Higher acid concentrations yielded more dissolved magnesium and iron in all acids tested, except for acetic acid. Ammonium salt solutions were the only solvents tested that extracted magnesium selectively, but the extraction ratio was much lower than the extraction achieved using acids. Neither of the alkaline solutions tested (sodium hydroxide, potassium hydroxide nor ammonia) managed to dissolve any measurable amount of magnesium or iron.

Reaction temperature was found to have a large effect on the dissolution of serpentinite in all three mineral acids evaluated: the extraction of magnesium and iron increases with increasing reaction temperature and

residence time. However, very little silicon was dissolved (<4%). All of the three mineral acids evaluated managed to extract all magnesium in serpentinite at 70 °C in 2 h. Sulfuric acid extracted magnesium faster than hydrochloric acid, which in turn extracted magnesium faster than nitric acid. The magnetite in serpentinite was harder to dissolve than serpentine. Both sulfuric acid and hydrochloric acid were more efficient than nitric acid at extracting iron from serpentinite.

The activation energies determined for magnesium extraction with mineral acids were approximately the same thus suggesting that the same mechanism was at work. The dissolution kinetics were found to follow rather well a shrinking core model for constant particle size with product diffusion as the rate-controlling step for all three mineral acids tested. The low concentration of dissolved silicon indicates that silicon stays on the particle while magnesium and iron is extracted. The high activation energy indicates that the chemical reaction initially controls the rate, with product layer diffusion gradually becoming rate limiting as it builds up. While product layer diffusion explains the dissolution mechanism for a particle size distribution of 74–125 µm, another mechanism seems to be rate limiting for particles of 125–500 µm.

Although the experiments show that common mineral acids can extract magnesium from serpentinite in time frames relevant for industrial processes, a successful carbonation process must also manage to precipitate magnesium carbonate and recycle most of the additional chemicals used. Therefore, more research on process development is needed before serpentinites can be used for long-term storage of CO₂.

Explanation of symbols

Symbol	Meaning	Unit
b	Stoichiometric coefficient	[–]
c_i	Mass concentration of i	[mg l ⁻¹]
C_i	Molar concentration of i	[mol cm ⁻³]
D_e	Effective diffusion coefficient in a porous structure	[cm ² s ⁻¹]
k	Reaction rate constant	[s ⁻¹]
K_0	Frequency factor	[s ⁻¹]
E	Activation energy	[J mol ⁻¹]
m	Mass	[mg]
m_i/m	Mass fraction of element i	[mg g ⁻¹]
ρ	molar density	[mol cm ⁻³]
R	Ideal gas constant: 8.3145	[J K ⁻¹ mol ⁻¹]
R^2	Multiple regression correlation coefficient	[–]
r	Radius of particle	[cm]
t	Reaction time	[s]
T	Temperature	[K]
V	Volume	[l]
X_i	Converted fraction of i	[–]

Acknowledgements

We thank Esko Pöyliö and Rita Kallio at Ruukki for generously providing us with XRF and XRD services, and the Laboratory of Energy Engineering and Environmental Protection for facilitating this work. We thank Mika Järvinen for helpful comments and proof-reading, and Jaakko Savolahti for assisting us with the experiments. We acknowledge the Nordic Energy Research, the Finnish Funding Agency for Technology and Innovation (TEKES) and the Finnish Recovery Boiler Committee for financial support. Ron Zevenhoven acknowledges the Academy of Finland for an Academy Researcher position (2004–2005).

References

- Apostolidis, C.I., Distin, P.A., 1978. The kinetics of the sulphuric acid leaching of nickel and magnesium from reduction roasted serpentine. *Hydrometallurgy* 3, 181–196.
- Blencoe, J.G., Palmer, D.A., Anovitz, L.M., Beard, J.S., 2004. Carbonation of metal silicates for long-term CO₂ sequestration; patent application WO 2004/094043.
- Chen, Y., Brantley, S.L., 2000. Dissolution of forsteritic olivine at 658C and 2-pH-5. *Chem. Geol.* 165, 267–281.
- Fouda, M.F.R., Amin, R.E.-S., Abd-Elzaher, M.M., 1996a. Extraction of magnesia from Egyptian serpentine ore via reaction with different acids. I. Reaction with sulfuric acid. *Bull. Chem. Soc. Jpn.* 69 (7), 1907–1912.
- Fouda, M.F.R., Amin, R.E.-S., Abd-Elzaher, M.M., 1996b. Extraction of magnesia from Egyptian serpentine ore via reaction with different acids. II. Reaction with nitric and acetic acids. *Bull. Chem. Soc. Jpn.* 69 (7), 1913–1916.
- Goff, F., Lackner, K.S., 1998. Carbon dioxide sequestering using ultramafic rocks. *Environ. Geosci.* 5 (3), 89–101.
- Goldberg, P., Zhong-Ying, C., O'Connor, W.K., Walters, R.P., 2001. CO₂ mineral sequestration studies in U.S. *Journal of Energy & Environmental Research*, vol. 1, No. 1. U.S. Department of Energy (Available from: http://www.netl.doe.gov/publications/journals/jeer_toc.html [Accessed 4.8.2006]).
- Huijgen, W.J.J., Comans, R.N.J., 2003. Carbon Dioxide Sequestration by Mineral Carbonation. Energy Research Centre of the Netherlands (ECN). (Report Number ECN-C-03-016. Available from: <http://www.ecn.nl> [Accessed 27.7.2005]).
- Huijgen, W.J.J., Comans, R.N.J., 2005. Carbon Dioxide Sequestration by Mineral Carbonation—Literature Review Update 2003–2004. Energy Research Centre of the Netherlands (ECN). (Report number ECN-C-05-022. Available from: <http://www.ecn.nl> [Accessed 3.11.2005]).
- Hänchen, M., Prigiobbe, V., Storti, G., Seward, T.M., Mazzotti, M., 2006. Dissolution kinetics of forsteritic olivine at 90–150 °C including effects of the presence of CO₂. *Geochim. Cosmochim. Acta* 70, 4403–4416.
- IPCC, 2005. IPCC special report on carbon dioxide capture and storage. In: Metz, B., Davidson, O., de Coninck, H.C., Loos, M., Meyer, L.A. (Eds.), Prepared by Working Group III of the Intergovernmental Panel on Climate Change. Cambridge University Press, Cambridge.
- Jonckbloedt, R.C.L., 1998. Olivine dissolution in sulphuric acid at elevated temperatures — implications for the olivine process, an

- alternative waste acid neutralizing process. *J. Geochem. Explor.* 62, 337–346.
- Lackner, K.S., 2003. A guide to CO₂ sequestration. *Science* 300, 1677–1678.
- Lackner, K.S., Wendt, C.H., Butt, D.P., Joyce, E.L., Sharp, D.H., 1995. Carbon dioxide disposal in carbonate minerals. *Energy* 20 (11), 1153–1170.
- Levenspiel, O., 1972. *Chemical Reaction Engineering*, second ed. John Wiley & Sons, New York.
- Luce, R.W., Bartlett, R.W., Parks, G.A., 1972. Dissolution kinetics of magnesium silicates. *Geochim. Cosmochim. Acta* 36, 35–50.
- Maroto-Valer, M.M., Zhang, Y., Kuchta, M.E., Andréßen, J.M., Fauth, D.J., 2005. Process for sequestering carbon dioxide and sulphur dioxide. US Patent US2005/0002847.
- Park, A.-H.A., Fan, L.-S., 2004. CO₂ mineral sequestration: physically activated dissolution of serpentine and pH swing process. *Chem. Eng. Sci.* 59, 5241–5247.
- Park, A.-H.A., Jadhav, R., Fan, L.-S., 2003. CO₂ mineral sequestration: chemically enhanced aqueous carbonation of serpentine. *Can. J. Chem. Eng.* 81, 885–890.
- Pelmenschikov, A., Strandh, H., Pettersson, L.G.M., Leszczynski, J., 2000. Lattice resistance to hydrolysis of Si–O–Si bonds of silicate minerals: ab initio calculations of a single water attack onto the (001) and (111) β -cristobalite surfaces. *J. Phys. Chem., B* 104, 5779–5783.
- Teir, S., Aatos, S., Kontinen, A., Zevenhoven, R., Isomäki, O.-P., 2006. Silikaattimineraalien Karbonoiminen Hiilidioksidin Loppusijoitusmenetelmänä Suomessa (Silicate Mineral Carbonation as a Possible Sequestration Method of Carbon Dioxide in Finland). Finnish Association of Mining and Metallurgical Engineers, pp. 40–46 (Materia 1/2006).
- Teir, S., Eloneva, S., Fogelholm, C.-J., Zevenhoven, R., 2007. Dissolution of steelmaking slags in acetic acid for precipitated calcium carbonate production. *Energy* 32 (4), 528–539.
- Yogo, K., Teng, Y., Yashima, T., Yamada, K., 2004. Development of a new CO₂ fixation/utilization process (1): recovery of calcium from steelmaking slag and chemical fixation of carbon dioxide by carbonation reaction. Poster Presented at the 7th International Conference on Greenhouse Gas Control Technologies (GHGT-8) in Vancouver, BC, Canada, 5–9 September 2004.